

Effect of corrosion on the buckling capacity of tubular members

F H Øyasæter*, A Aeran, S C Siriwardane and O Mikkelsen

Department of Mechanical and Structural Engineering and Materials Science,
University of Stavanger, Norway

*Contact author: fridtjof@bergoya.no

Abstract. Offshore installations are subjected to harsh marine environment and often have damages from corrosion. Several experimental and numerical studies were performed in the past to estimate buckling capacity of corroded tubular members. However, these studies were either based on limited experimental tests or numerical analyses of few cases resulting in semi-empirical relations. Also, there are no guidelines and recommendations in the currently available design standards. To fulfil this research gap, a new formula is proposed to estimate the residual strength of tubular members considering corrosion and initial geometrical imperfections. The proposed formula is verified with results from finite element analyses performed on several members and for varying corrosion patch parameters. The members are selected to represent the most relevant Eurocode buckling curve for tubular members. It is concluded that corrosion reduces the buckling capacity significantly and the proposed formula can be easily applied by practicing engineers without performing detailed numerical analyses.

1. Introduction

Offshore structures are subjected to a very harsh and corrosive environment during their lifetime [1]. Corrosion is a major hazard for offshore structures, especially for structures in the splash zone [2]. Corrosion, as a time-dependent degradation process is highly relevant to aging offshore structures [3]. Ageing is becoming an increasing concern in the offshore industry and the majority of fixed offshore platform on the Norwegian Continental Shelf (NCS) and United Kingdom Continental Shelf (UKCS) are currently being operated beyond the design life [4]. It is therefore important to investigate the effect of structural degradation on the buckling capacity of aging offshore installations.

Structural degradation can occur in many forms but is mainly characterized by corrosion and reduction of member thickness with time. Corrosion is one of the major structural degradation phenomenon especially in the marine environment and can reduce the buckling capacity of members [5]. Corrosion can broadly be classified into localized and uniform corrosion. Localized corrosion such as crevice and pitting may not have a significant effect on the overall strength but can cause local stress concentrations and fatigue cracking [5]. Uniform is the most common form of corrosion [6] and causes uniform reduction of member thickness. Corrosion of offshore structures is normally counteracted using protective coating or a cathodic protection system (CPS) consisting of several sacrificial anodes. Also, a corrosion allowance is generally taken for the members in the splash zone where the rate of corrosion is the highest [3]. However, CPS has a typical life of only 5 to 15 years [5] and is ineffective in the



splash zone due to intermittent action of waves and tides [4]. Moreover, the maintenance and repair of CPS for fixed offshore structures are generally very costly and sometimes impractical [7]. In addition, the corrosion allowance is normally taken for the initial design life and not for the extended life, as is the case with ageing offshore structures [8].

Tubular members are often used to construct the primary load bearing system of offshore structures, especially for bottom fixed jacket structures and wind turbines [9]. The advantage of tubular members is low drag resistance and higher utilization of bearing capacity against the self-weight. The effect of corrosion on the ultimate load capacities of tubular members has become a growing concern [1]. Over the past decades, a significant amount of research has been carried out on the buckling capacity of corroded tubular members. Ostapenko et al. [10] studied the residual strength of corroded and dented tubular members by conducting test on several salvaged, fabricated, and small-scale manufactured column specimens. A procedure to estimate corroded cross-sections for local buckling was also proposed. Ostapenko and Gulec [11] analyzed the effect of multiple corrosion patches on the buckling capacity of tubular members and proposed a simplified procedure for estimating the capacity of such members. Lutes et al. [12] assessed the residual strength of corroded tubular using approximate formulas given by the American Petroleum Institute (API) [13]. These formulas consider global buckling accounting for inelasticity. Hebor and Ricles [1] carried out an analytical and experimental study of the strength of patch-corroded short tubular steel bracing members. The result of this study was used to derive a semi-empirical formula for estimating the strength of such members.

Okada et al. [14] investigated the deterioration of strength of tubular members with perforation due to corrosion and proposed a simplified method to estimate the residual strength of such members. Yamane et al. [15] examined the ultimate strength of steel tubular members with uniform corrosion and patch corrosion under coating paint, both numerically and experimentally. The applicability of existing design formulas for finding residual strength was also examined. Nazari et al. [9] investigated the strength of patch corroded tubular members and performed a parametric study for the different parameters describing a corrosion patch. A semi-empirical formula to predict the capacity was derived. Most of the proposed formulas in previously mentioned studies are semi-empirical. These semi-empirical relations were either proposed based on very limited experimental data or using results from numerical analyses on a few cases. Moreover, most of the earlier proposed formulas does not considered the effect of initial imperfections for assessing the buckling capacity of corroded tubular members.

In addition to research articles, several codes are available for assessment of existing structures [16] [17]. These assessment codes recommend uniform thickness wastage of the member surface. However, corrosion located in some parts of the member can be more critical for buckling capacity due to the load eccentricity induced by such patch corrosion. There are no generalized guidelines available for finding the buckling capacity of tubular members subjected to patch corrosion. Also, it is computationally demanding and time consuming for practicing engineers to model patch corrosion in detail to assess the buckling capacity of these tubular members. It is therefore necessary to have an accurate analytical formula to determine the buckling capacity of corroded tubular members which can be easily applied by practicing engineers, without performing advanced numerical analyses.

This paper proposes a new analytical formula for estimating the buckling capacity of corroded tubular members. This formula also includes the effect of initial geometrical imperfections and can be applied to members subjected to uniform corrosion. The proposed formula is verified using result from finite element analysis (FEA) performed on several corroded members having different combinations of patch corrosion. One of the most relevant buckling curve from Eurocode 3 (EC 3-1-1) [18] for hollow cross-sections is used as reference for comparing results from corroded and uncorroded tubular members. This buckling curve is reproduced using finite element (FE) simulation results from a set of uncorroded tubular members. The paper starts by discussing the relevant Eurocode buckling curve for uncorroded tubular members and deriving it using results from FEA. Then, the procedure for performing nonlinear buckling analyses using FEA on corroded tubular members is explained and the result from a study of corrosion patch parameters is presented. Next, the proposed formula is derived and presented in detail. Finally, the verification study of the proposed formula is presented.

2. Eurocode buckling curves for uncorroded tubular members

The Eurocode buckling curves consider flexural buckling of columns with initial imperfections and is used to find buckling capacity resistance of columns according to EC 3-1-1. The various initial imperfections are represented using a single equivalent imperfection with sinusoidal shape [18]. The different buckling curves represent different values for the amplitude of this sinusoidal shaped imperfection.

Buckling curve “a” given in EC 3-1-1 [18] represents hollow cross-sections with yield stress (f_y) less than 460 MPa that has been produced by hot-rolling [19]. This is one of the most relevant curves for tubular members used in offshore structures and is therefore used as a reference for comparing the buckling capacity for uncorroded and corroded tubular members.

2.1. Considered cases of tubular members

Curve “a” is derived using results from FEA of a set of uncorroded members. The set consist of eight members with different values for relative slenderness ($\bar{\lambda}$) and is selected to represent buckling curve “a”. Table 1 shows the dimensions such as diameter (D), thickness (t) and length (L) of these members. The cross-sectional class and relative slenderness ($\bar{\lambda}$) of the selected tubular members are also shown. Each value of relative slenderness has a corresponding value for the reduction factor (χ). The reduction factor (χ) is multiplied with the axial yield capacity to find the flexural buckling capacity.

Table 1. Dimensions of the selected tubular members

No.	D (mm)	t (mm)	L (m)	Class	$\bar{\lambda}$
1	1800	35	14.307	3	0.3
2	1800	35	19.076	3	0.4
3	1200	30	18.971	2	0.6
4	1200	30	25.294	2	0.8
5	1000	40	25.957	1	1.0
6	1000	40	31.148	1	1.2
7	500	35	20.156	1	1.6
8	500	35	25.195	1	2.0

The buckling curve “a” given in EC 3-1-1 [18] and the corresponding slenderness ratios/points of eight selected member geometries on the curve is shown in Figure 1. The selected members have a relative slenderness ranging from 0.3 to 2.0. Values between 2.0 and 3.0 are excluded to only represent the “usable” part of the buckling curve. The curve “a” is only valid for members with cross-sectional classes 1, 2 and 3 that are subjected to global/flexural buckling.

2.2. Finite element analysis of uncorroded members

Initial imperfections are included as a single geometrical imperfection with sinusoidal shape. This imperfection is introduced by first performing an eigenvalue buckling analysis of each of the uncorroded members, which result in a large sinusoidal shaped deformation of the members and finally scaling the deformation to achieve the same amplitude of the initial imperfections as in EC 3-1-1 [18]. Figure 2 shows the deformed shape after performing an eigenvalue buckling analysis.

The selected material is steel grade of S355 and material properties are given in Table 2. The material behavior is assumed to be elastic-perfectly plastic. The members are modelled as pinned-ended columns and loaded by controlling displacement. The members are meshed as a single body using the sweep-

method in ANSYS version 17.2. This method creates a hexahedral mesh, where the number of nodes and elements is much less than if a free meshing method is applied, which makes it very efficient [20]. The element type is SOLID186 (i.e. 20-node brick element) [20] and element size is set based on a mesh convergence study.

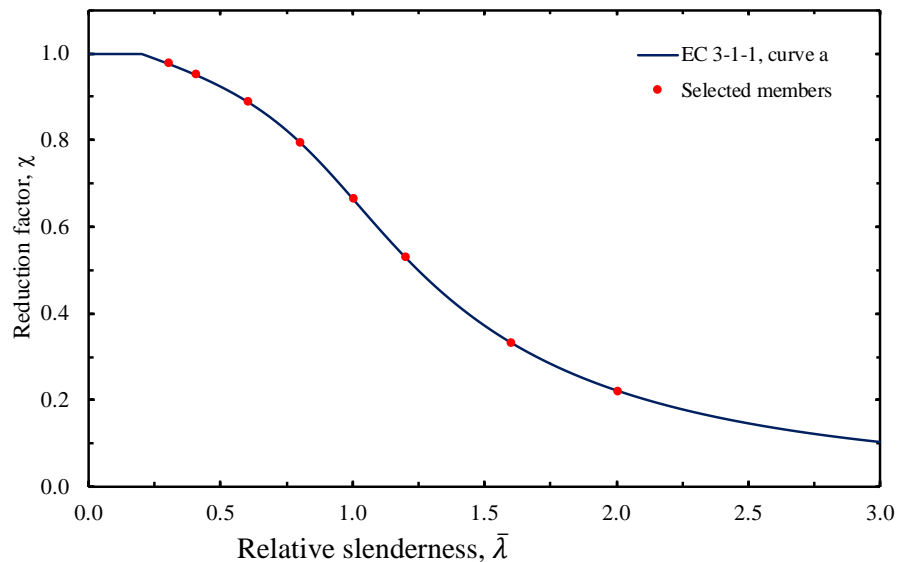


Figure 1. Eurocode buckling curve “a” with selected members indicated along the curve

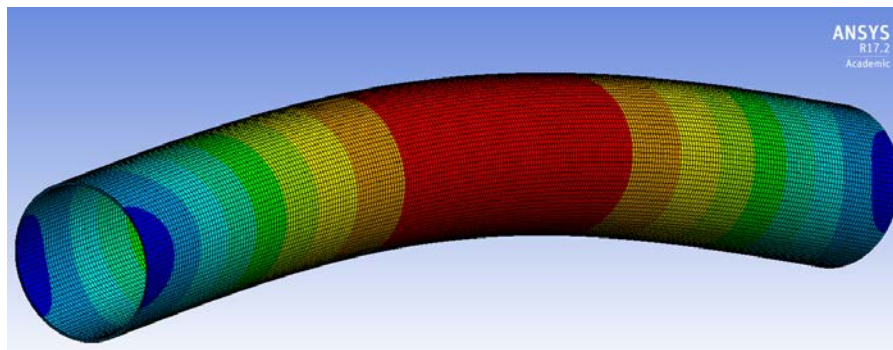


Figure 2. Deformation of a tubular member subjected to Euler's critical buckling load in an eigenvalue buckling analysis

Table 2. Material properties of reference material

Steel type	Yield stress (MPa)	Young' modulus (MPa)	Poisson's ratio
S355	355	210000	0.3

2.3. Comparison of EC buckling curves with FEA results

The nonlinear buckling analysis is performed for each of the considered members shown in Table 1. The results are used to reproduce buckling curve using ANSYS employed FE simulations. Figure 3 shows both the reproduced buckling curve and the buckling curve from EC 3-1-1 [18]. The maximum deviation between the two curves is around 2 %, where buckling curve from EC 3-1-1 [18] gives slightly lower buckling capacity than from FEA.

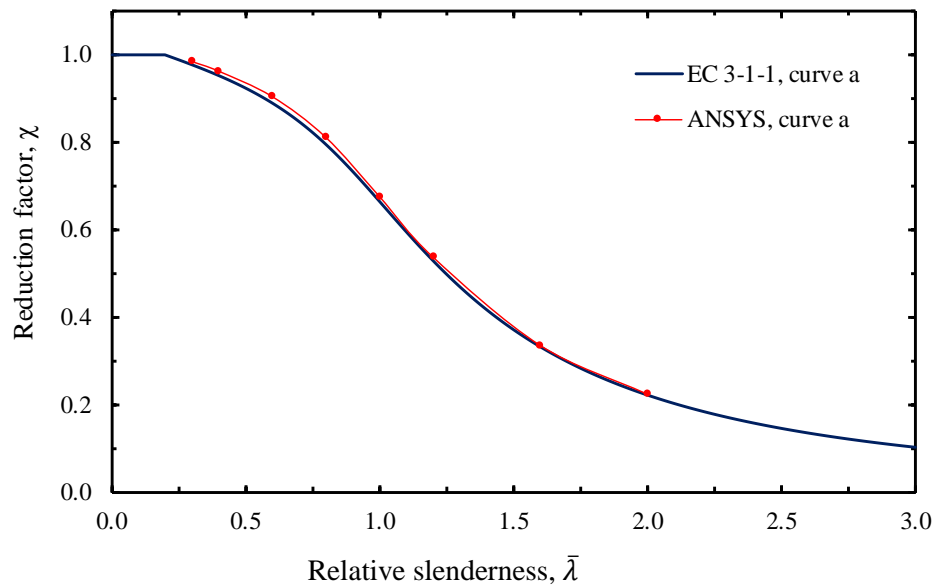


Figure 3. Buckling curve “a” using analytical formulas from EC 3-1-1 [18] and FE-analysis in ANSYS

3. Finite element analysis of corroded tubular members and parametric study of corrosion patch parameters

This section describes the procedure for modelling corroded tubular members and performing nonlinear FEA on these members using ANSYS. The result from a study of the corrosion patch parameters is also presented. The aim this study is to investigate the effect of patch parameters on buckling capacity of corroded tubular members. The corrosion patch is conservatively assumed to be rectangular shaped by combining several irregular shaped patches.

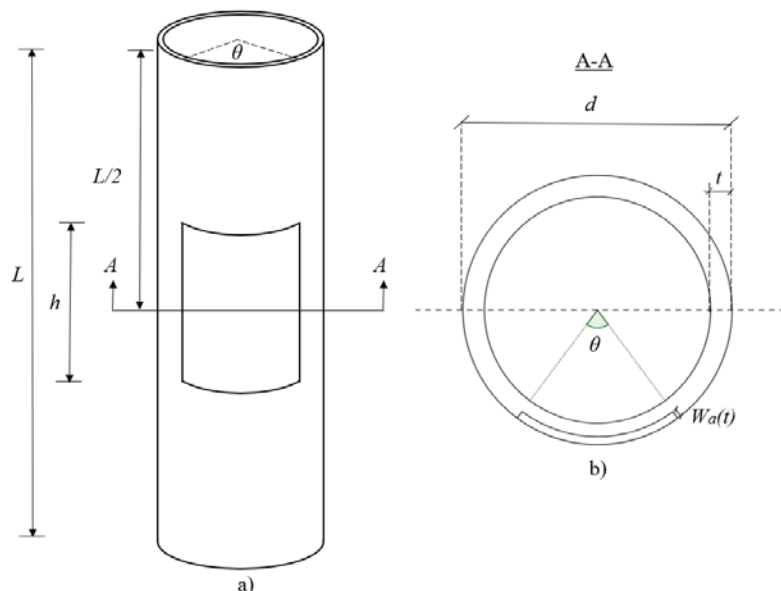


Figure 4. Schematic representation of corroded tubular members: a) Tubular member with a corrosion patch. b) Cross-section at mid-span

The patch can be described by three different parameters. These are height (h), angular extent (θ) and the thickness wastage (W_a). Figure 4 show a tubular member with outer diameter (d), wall thickness (t) and a corrosion patch centered in the mid-span.

3.1. Corrosion wastage model

The thickness wastage from corrosion is found using a recently proposed corrosion wastage model [5]. The model is given in equation (1):

$$W_a(t) = R_{corr} \alpha (t - t_{pt}) \quad (1)$$

where, $W_a(t)$ is the thickness wastage as a function of time, R_{corr} is the rate of corrosion (mm/year), α is parameter that is equal to 1 or 2 depending if the corrosion is one-sided or two-sided, t is the time in years and t_{pt} is the corrosion protection time in years. The corrosion rate (R_{corr}) in the splash zone is taken as 0.3 mm/year according to design standards [21]. Thickness wastage can also be expressed as an equivalent number of years (or age).

3.2. Modelling of corroded members in ANSYS

The models of the tubular members to be used in the nonlinear buckling analyses include both the sinusoidal shaped initial imperfection and the corrosion patch. The corrosion patch is assumed to be positioned at the outer surface (single-sided corrosion) at the mid-span of the tubular member. Circumferentially, the patch is placed in the opposite direction of the lateral deflection from the initial imperfection.

3.2.1. Modelling of corrosion patch

The corrosion patch is modelled using the CAD-software SolidEdge. The patch is first projected onto the surface of the member and then created using a cut-out tool in SolidEdge, as shown in Figure 5.

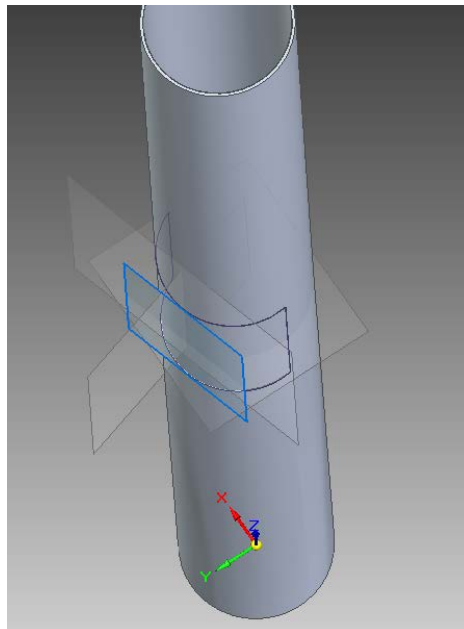


Figure 5. Modelling corrosion patch on a tubular member

3.2.2. Meshing procedure

The initial imperfection and corrosion patch, results in a very irregular shape that it is not possible to mesh as a single body using the “sweep-method”. Instead, the geometry of the tubular members is split

into “sweepable” bodies, as shown in Figure 6. The “sweepable” bodies are mostly meshed with SOLID186 and SOLID187 (i.e. 10-node tetrahedral element). The two mentioned element types support both geometric and material non-linearities [20].

The optimal element size is determined by performing a convergence study. The convergence study is limited to varying element size in the “sweepable” bodies and using a fixed element size in the small intermediate body. The geometry of a corroded tubular member consists of four different “sweepable” bodies. Two cylindrical bodies in each end of the tubular member and two half cylinders in the corroded part of tubular member. The two bodies in the corroded parts is meshed with a finer mesh than the two bodies in each end. Table 3 shows the different combination of mesh sizes and results from the mesh convergence study where the critical load is taken as the axial load that initiates yielding. The mesh convergence study is performed on the first member from Table 1. The corrosion patch had a height $h = L/2$, angle $\theta = 180^\circ$ and wasted thickness $W_a = 7.5$ mm. Case 3 from Table 3 is selected as a combination of mesh sizes.

Table 3. Critical buckling load for different combinations of mesh sizes

Case	Mesh size (mm), end bodies	Mesh size (mm), bodies in corroded part	Critical load (MN)
1	300	150	54.028
2	200	100	53.950
3	100	50	53.689
4	80	40	53.523
5	60	30	53.534

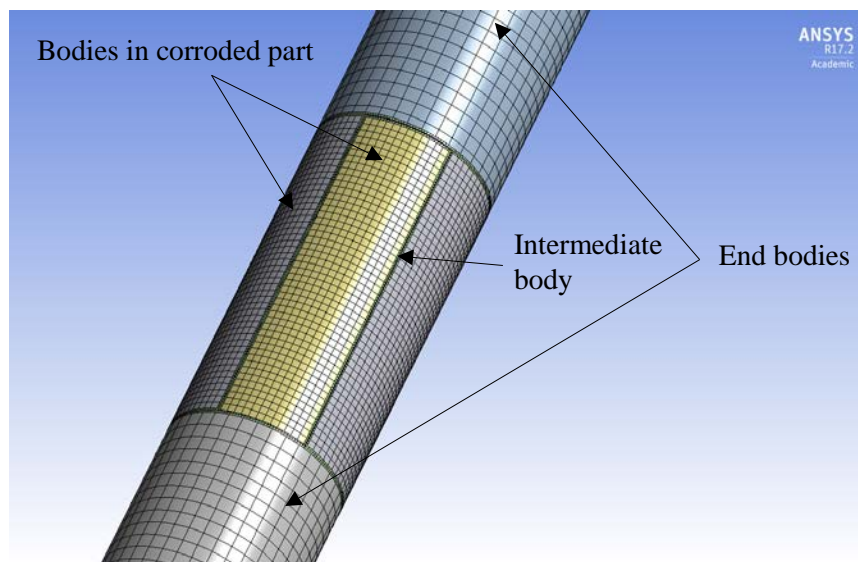


Figure 6. FE mesh of a corroded member (member split into multiple bodies)

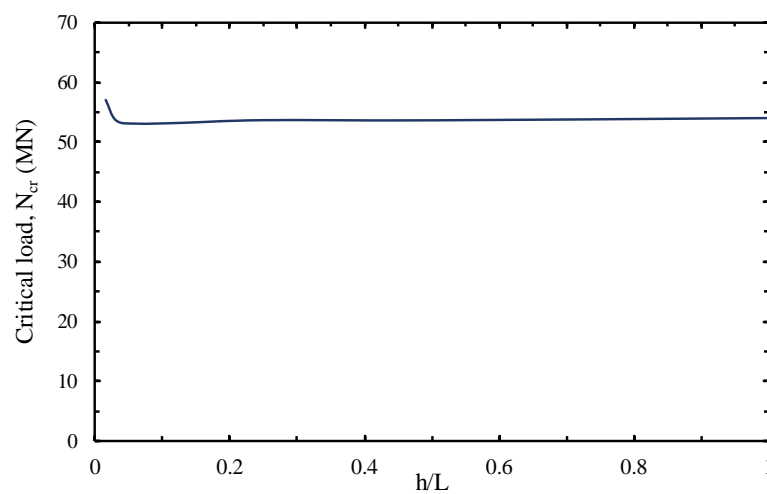
3.3. Considered cases for parametric study

The aim of this parametric study is to investigate the effect of corrosion patch parameters (W_a , h and θ) on the buckling capacity of a tubular member. It is also an aim to find the most critical position of the patch on the tubular member. The study is carried out by varying the value of each patch parameter, keeping the two other parameters constant and performing a FEA for each case. All testing of patch parameters is done on the same member, which is the first of the selected member in Table 1. Each of the test is given a test number and all the results are listed in Table 4.

Table 4. Result from corrosion patch parameter testing

Parameter	Test No.	h/L	θ ($^\circ$)	W_a (mm)	N_{cr} (MN)
h	1	1	180	7.5	54.069
	2	1/2	180	7.5	53.693
	3	1/4	180	7.5	53.717
	4	1/8	180	7.5	53.262
	5	1/16	180	7.5	53.145
	6	1/32	180	7.5	53.653
	7	1/64	180	7.5	57.066
θ	8	1/4	30	7.5	64.738
	9	1/4	60	7.5	61.650
	10	1/4	120	7.5	56.072
	11	1/4	180	7.5	53.717
	12	1/4	360	7.5	49.899
W_a	13	1/4	180	1.5	65.069
	14	1/4	180	4.5	59.937
	15	1/4	180	7.5	53.693
	16	1/4	180	10.5	47.073
	17	1/4	180	13.5	41.014

3.3.1. *Effect of corrosion patch height on the critical load.* The result from testing the effect of height on the critical load is plotted and shown in Figure 7. It can be seen that the critical load is almost independent of the corrosion patch height.

**Figure 7.** Variation of critical load with height of corrosion patch

3.3.2. Effect of corrosion patch angle on the critical load. Figure 8 shows the way critical load varies with angular extent of the corrosion patch. It can be seen that the load is very dependent on the angular extent of the corrosion patch. This shows that increasing angle results in a lower buckling capacity.

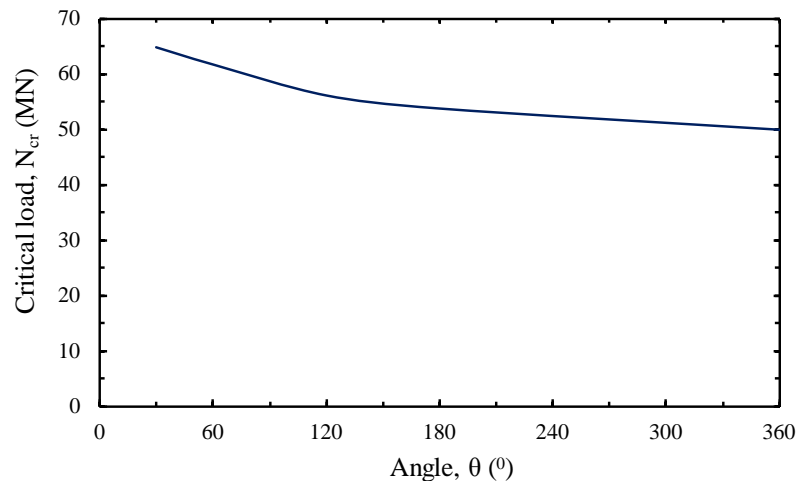


Figure 8. Variation of critical load with the corrosion patch angle

3.3.3. Effect of corrosion thickness wastage on the critical load. The variation of the critical load with different values for thickness wastage is plotted in Figure 9. It can be seen that the critical load is significantly dependent on the wasted thickness of the corrosion patch and indicates a linear relationship between these two parameters.

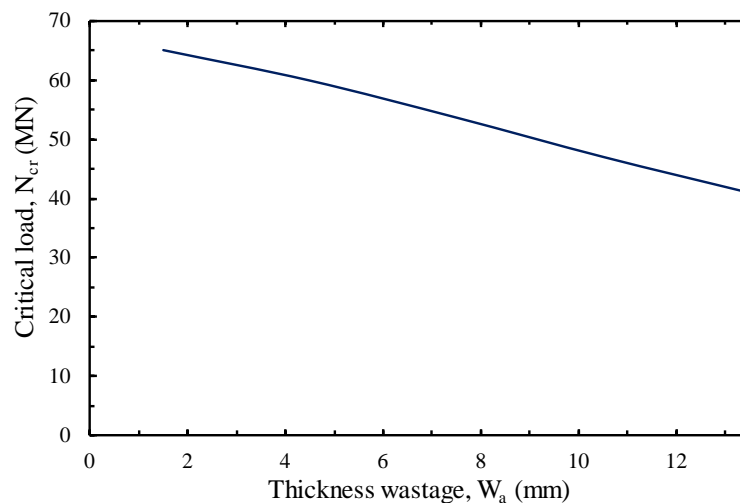


Figure 9. Variation of critical load with thickness wastage of corrosion patch

3.3.4. Critical position of the corrosion patch. As mentioned earlier, the initial imperfections are represented by a single equivalent imperfection with a maximum value of load eccentricity in the mid-span. The most critical position of the corrosion patch is theoretically when the patch is centered at the mid-span of the member. This has been confirmed in a study by Nazari et al. [9] and therefore not tested any further here. The corrosion patch can be placed anywhere around the circumference of the cross-section. The maximum eccentricity of corroded cross-section can be achieved when the corrosion patch is located most far away from initial longitudinal axis of the member.

The maximum eccentricity governs the buckling capacity of the corroded tubular member. Two different positions are tested using results from FEA. The position where the corrosion patch is located

most away from initial longitudinal axis is called “back” and the position where it is placed nearest is called “front”. The two back and front side positions have been tested for three different cases and the results are shown in Table 5. The results show that the most critical position of the patch is located circumferentially opposite side of the initial geometric imperfection (“back”) and thus most far away from initial longitudinal axis. This position is used for modelling corrosion for the verification study in the Section 5. Figure 10 shows a tubular member with a corrosion patch located at his position.

Table 5. Result from testing of patch position

d (m)	t (mm)	L (m)	θ ($^\circ$)	W_a (mm)	h/L	Critical load, N_{cr} (MN)	
						Back side	Front side
1.8	35	14.307	180	7.5	0.5	53.693	55.074
1.8	35	14.307	180	7.5	0.25	53.717	55.582
0.5	35	20.156	180	7.5	0.5	3.4190	3.7709

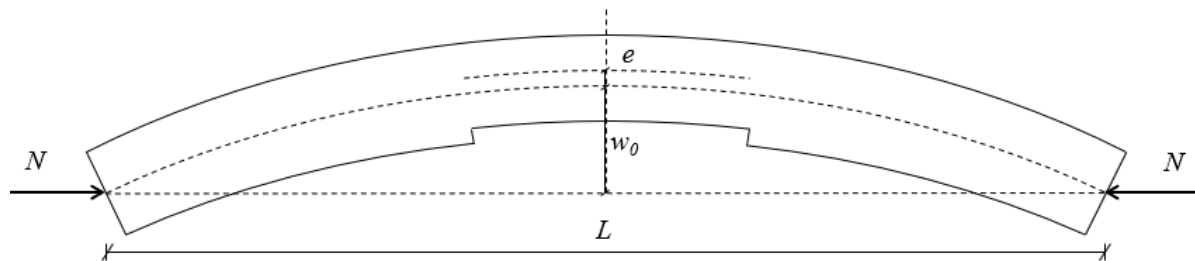


Figure 10. Tubular member with an equivalent initial imperfection and a corrosion patch centred at the mid-span and on the “back” position.

4. Derivation of formula for estimating buckling capacity of corroded tubular members

This paper derives a new formula to include the effect of corrosion on the buckling capacity of tubular steel members. The proposed formula considers a tubular member with a single rectangular shaped patch of uniform corrosion centered at the mid-span, as shown in Figure 4. The patch is described by the height (h), angular extent (θ) and the thickness wastage (W_a) as described in the previous section. Initial imperfections are included by assuming that the member have an equivalent geometrical imperfection with sinusoidal shape. The corrosion patch is centered at the mid-span of the member because the initial bending stresses from the initial imperfection has a maximum value at the mid-span and this will be the critical cross-section (i.e. most stresses cross-section). The corrosion patch is positioned in the opposite direction of the lateral deflection to have maximum eccentricity of the axial load, resulting in maximum stresses. The formula is derived on the assumptions of linear elastic material behavior and corresponding failure occurs when the most heavily loaded cross-section reaches yield strength of the material.

4.1. Cross-sectional properties of corroded tubular members

A corroded cross section where W_a is the thickness wastage, θ is the angular extent and e is the shifted distance of the neutral axis is shown in Figure 11. The neutral axis is shifted because the corrosion patch leads to non-uniform reduction of cross-sectional area. The surface of the corrosion patch is assumed to be uniformly corroded.

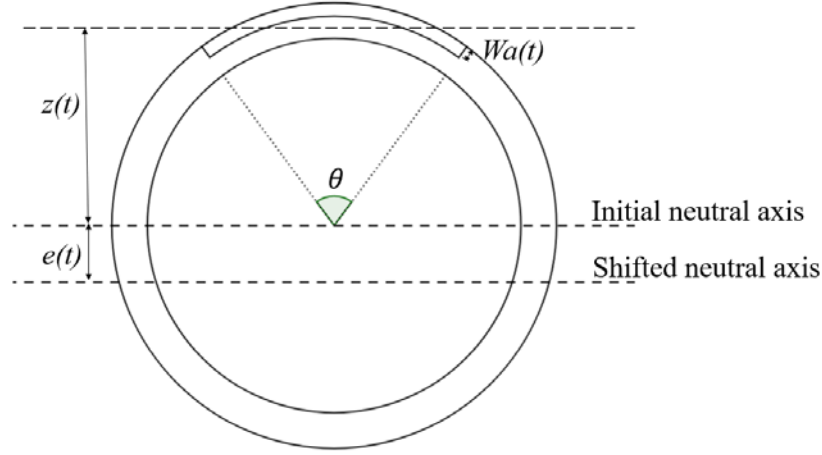


Figure 11. Cross-section of the corroded part of a tubular member

The reduced cross-sectional area as a function of time t is given in equation (2):

$$A_{red}(t) = L_{red} W_a(t) \quad (2)$$

where L_{red} is the arc-length of the corrosion patch and $W_a(t)$ is the thickness wastage. The distance from the neutral axis of the corrosion patch to the neutral axis of the original cross-section (z) is found using equation (3).

$$z(t) = \frac{d \sin\left(\frac{\theta}{2}\right)}{\theta_{rad}} \quad (3)$$

where A_{eff} is the effective area of the corroded cross-section. The effective moment of inertia can be found using equation (4).

$$I_{eff}(t) = I_0 + A_0 e(t)^2 - \left[\Delta I + A_{red} (z(t) + e(t))^2 \right] \quad (4)$$

where I_0 is the moment of inertia of the uncorroded cross-section, A_0 is the cross-sectional area of the uncorroded cross-section and ΔI is the moment of inertia of the corrosion patch. The section modulus of the corroded cross-section is found using equation (5):

$$W_{eff}(t) = \frac{I_{eff}(t)}{y_{max}(t)} \quad (5)$$

where y_{max} is the maximum distance from the neutral axis to the outmost fiber of the cross-section.

4.2. Derivation of proposed formula

The corrosion patch is positioned so that the initial imperfection (w_0) and the shifting of neutral axis (e) causes maximum stresses at the mid-span (as shown in Figure 9). The first order bending moment (M) in the mid-span is found using equation (6).

$$M = N(w_0 + e) \quad (6)$$

The second order bending moment in the mid-span is found by using the amplification factor (AF) according to EC 3-1-1 [18]. The amplification factor can be found using equation (7):

$$AF = \left(1 - \frac{N}{N_E}\right)^{-1} \quad (7)$$

where N_E is Euler's critical load found using corroded cross-sectional properties. AF is exact for the equivalent initial imperfection, but not for the shifting of neutral axis. As a simplification, the amplification factor in equation (7) is used for both the initial imperfection and the shifting of neutral axis. The total bending moment in the mid-span is found using equation (8):

$$M = N(w_0 + e) \left(1 - \frac{N}{N_E}\right)^{-1} \quad (8)$$

The following failure criteria is used for a tubular member with elastic material behavior subjected to combined loading:

$$\frac{N}{N_{Rk}} + \frac{M}{M_{Rk}} \leq 1.0 \quad (9)$$

where N_{Rk} is the characteristic axial load capacity and M_{Rk} is the characteristic bending moment capacity of the corroded cross-section. The failure criteria can be written as shown in equation (10):

$$\frac{N}{A_{eff} f_y} + \frac{N(w_0 + e) \left(1 - \frac{N}{N_E}\right)^{-1}}{W_{eff} f_y} \leq 1.0 \quad (10)$$

where f_y is the yield stress for the material used in the tubular member.

The critical axial load is found by solving equation (11) with respect to the unknown axial load (N). This results in a second order equation with the following possible solution:

$$N_{1,2} = \frac{1}{2W_{eff}} \left(A_{eff} N_E e + A_{eff} N_E w_0 + A_{eff} W_{eff} f_y + N_E W_{eff} \pm \sqrt{Z} \right) \quad (11)$$

$$\begin{aligned} Z = & A_{eff}^2 N_E^2 e^2 + 2A_{eff}^2 N_E^2 e w_0 + A_{eff}^2 N_E^2 w_0^2 + 2A_{eff}^2 N_E W_{eff} e f_y \\ & + 2A_{eff}^2 N_E W_{eff} f_y w_0 + A_{eff}^2 W_{eff}^2 f_y^2 + 2A_{eff}^2 N_E^2 W_{eff} e \\ & + 2A_{eff}^2 N_E^2 W_{eff} w_0 - 2A_{eff} N_E W_{eff}^2 f_y + N_E^2 W_{eff}^2 \end{aligned} \quad (12)$$

The critical load (N_{cr}) is the lowest load that satisfies the failure criteria given in Equation (11) and is the second solution of Equation (11). To simplify this equation, the following imperfection parameter is introduced:

$$\eta_{corr} = \frac{A_{eff}(e + w_0)}{W_{eff}} \quad (13)$$

The imperfections parameter is a modified version of the imperfection parameter from Perry-Roberson's equation [22]. Introducing this parameter into second solution in equation (11) result in formula with similar format as the Perry-Robertson's equation that takes corrosion into account:

$$N_{cr} = \frac{N_{Rk} + N_E(1 + \eta_{corr}) - \sqrt{(N_{Rk} + N_E(1 + \eta_{corr}))^2 - 4N_{Rk}N_E}}{2} \quad (14)$$

The proposed formula in Equation (14) can easily be used by practicing engineers to find the critical buckling capacity of corroded tubular members without the need for performing advanced numerical analyses.

5. Verification of proposed formula

The proposed formula is verified using result from FE-analyses of tubular members with different combinations of patch corrosion. The combinations are created by varying the values of the different corrosion patch parameters.

5.1. Selection of cases for verification study

The set of tubular members given in Table 1 is also used in the verification study. Curve “a” is therefore used for quantifying the effect of corrosion on the buckling capacity and to quantify the difference between result obtained from the proposed formula and the corresponding result from FEA. The material data from Table 2 is also used for the verification study. The effect of corrosion is studied by performing FE analyses for different cases of patch corrosion. As mentioned in Section III, corrosion case is a combination of values for the three different patch parameters (h , θ and W_a). The patch parameter study indicated that the critical load is independent of patch height. Therefore, the patch height is kept fixed to a value of 1/2 of the length of the tubular member. For the other two parameters, it is selected four different values for patch angle and four values for thickness wastage. Combining all these, 128 different corrosion cases of the tubular members are considered for nonlinear FEA. The values in Table 6 are selected based on the patch parameter study conducted in the Section 3.

Table 6. Overview of the number of FE analyses in the verification study

No. of members	θ	h	W_a (mm)	Age (years)	Number of analyses
8	60,	L/2	1.5,	10,	128
	180,		4.5,	20,	
	120,		7.5,	30,	
	380		10.5	40	

5.2. Comparison of results obtained from proposed formula and from FEA

The results of the verification study are presented as four different plots for the different values of the patch angle, as shown in Figure 12 to Figure 15. The plots show different buckling curves, where each curve represents a specific value of thickness wastage. Each of the plots presents the buckling curves from FEA results and corresponding curves obtained using the proposed formula. The buckling curves from the proposed formula are shown as a solid thick line and the buckling curves from FEA results is shown as dotted thin lines.

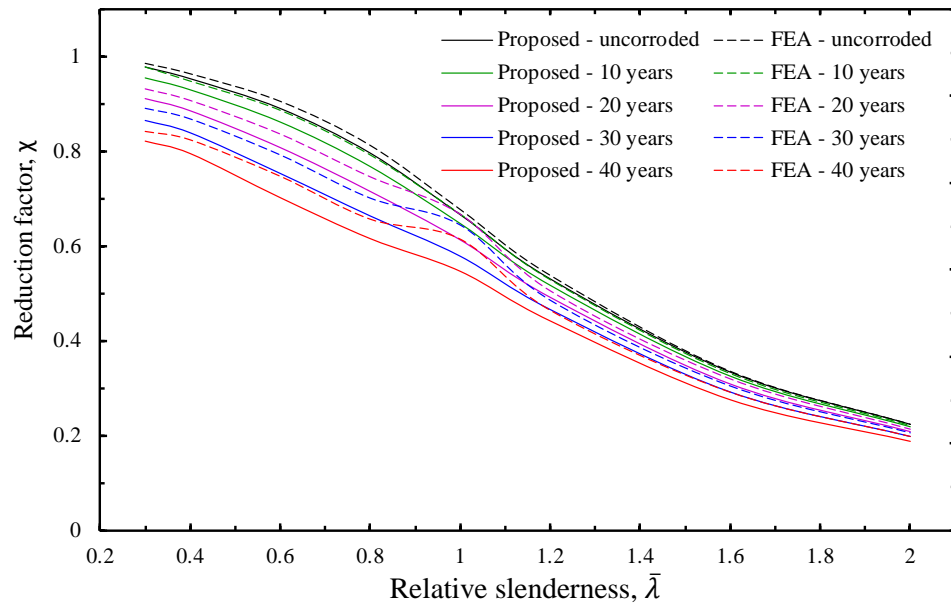


Figure 12. Comparison of results from FEA and using the proposed formula for $h = L/2$ and $\theta = 60^\circ$

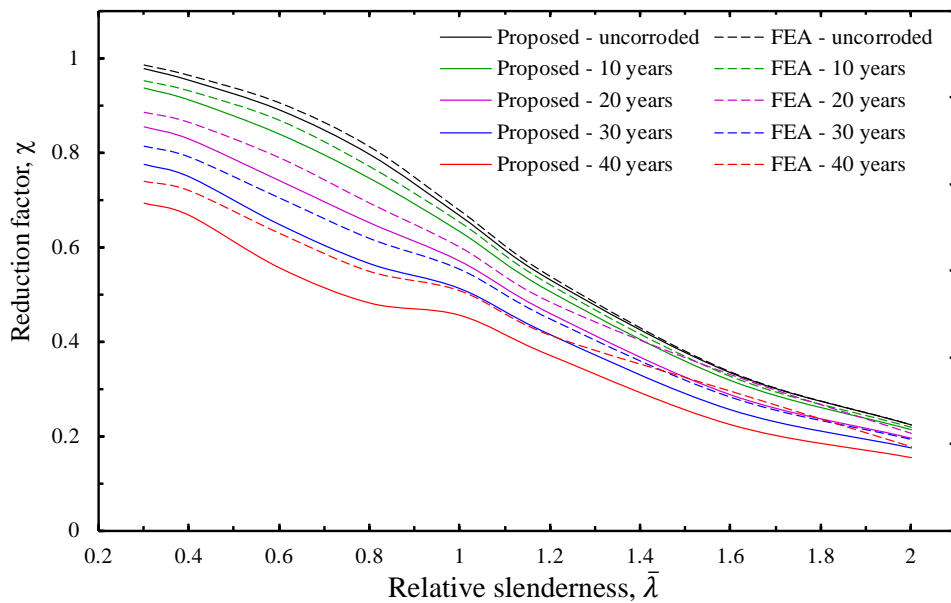


Figure 13. Comparison of results from FEA and using the proposed formula for $h = L/2$ and $\theta = 120^\circ$

5.3. Discussion of the results.

This section discusses the validity of the proposed formula for determining buckling capacities of corroded tubular members after comparing the results obtained by FEA. The effects of corrosion patch angle and thickness wastage on critical load are also discussed in the later part of the section.

5.3.1. Comparison of proposed formula and results from FEA. The critical load obtained from the proposed formula is always lower than the load from FEA, as shown in Figure 16. The deviation between result from FEA and the proposed formula seems to be at maximum at a patch angle of 180° and minimum at an angle of 360° . The maximum, minimum and average deviation is 22,7%, 0,8% and 6,1%

respectively. The deviation is possibly due to some degree of inelastic buckling in the FEA results, which is not considered in the proposed formula.

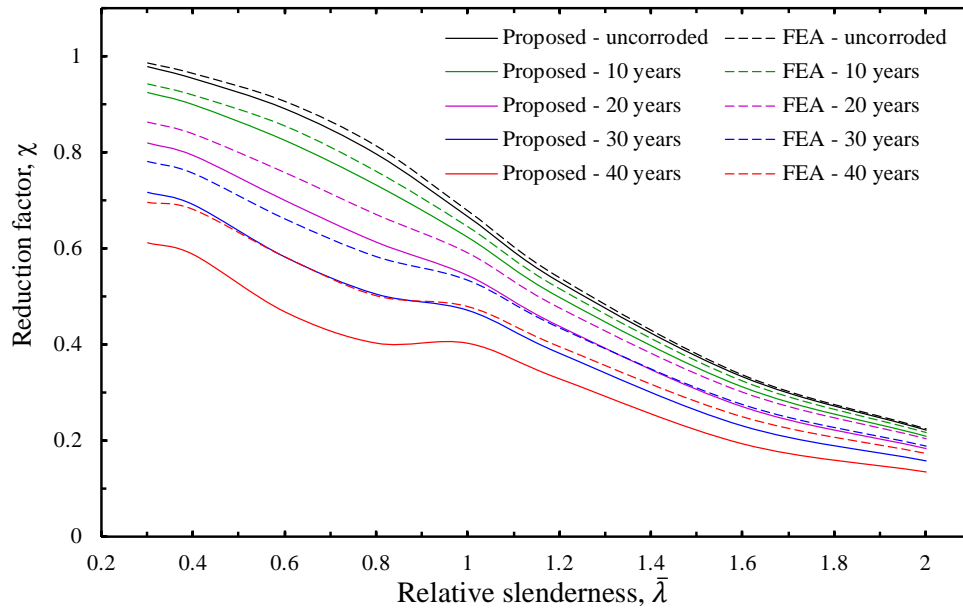


Figure 14. Comparison of results from FEA and using the proposed formula for $h = L/2$ and $\theta = 180^\circ$

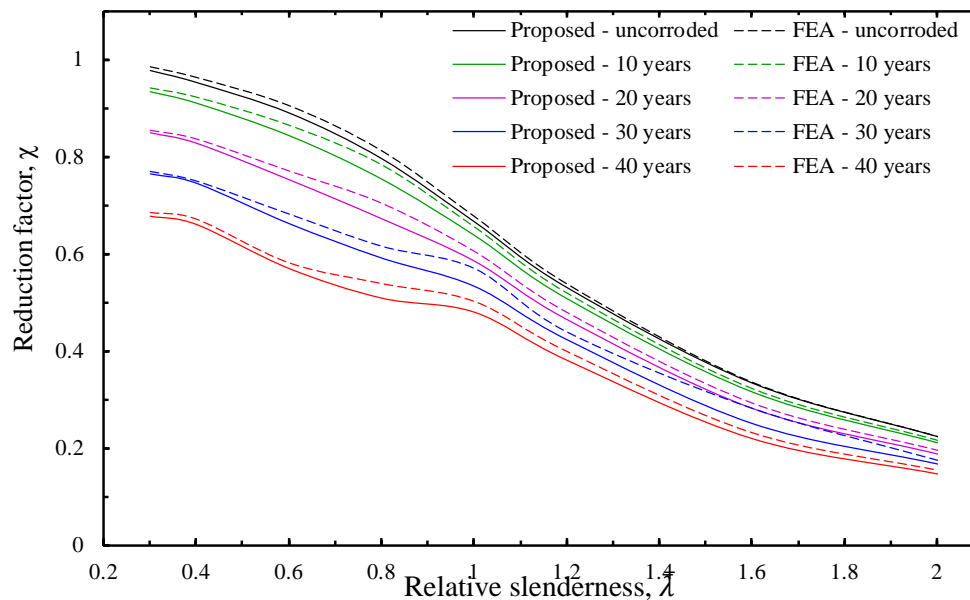


Figure 15. Comparison of results from FEA and using the proposed formula for $h = L/2$ and $\theta = 360^\circ$

5.3.2. Effect of corrosion patch angle on the critical load. The patch parameter study indicated that the critical load decreases with increasing angular extent (θ). The effect of patch angle is further investigated by comparing the buckling curves from different values for patch angle. This is done by keeping thickness wastage constant. The largest value for thickness wastage is selected for this comparison to maximize the differences between the curves. This resulted in a plot shown in Figure 17. An angular

extent of 120° is more critical than 60° . Also, an angle of 180° or 360° is more critical than 120° . Increasing the angular extent (θ) from 0° to 180° leads to both reduction of cross-sectional area and shifting of the neutral axis. The shift is reduced when increasing the angle 180° to 360° and is zero for angle equal to 360° . It can be concluded that increasing angle results a lower critical load for angles up to 180° .

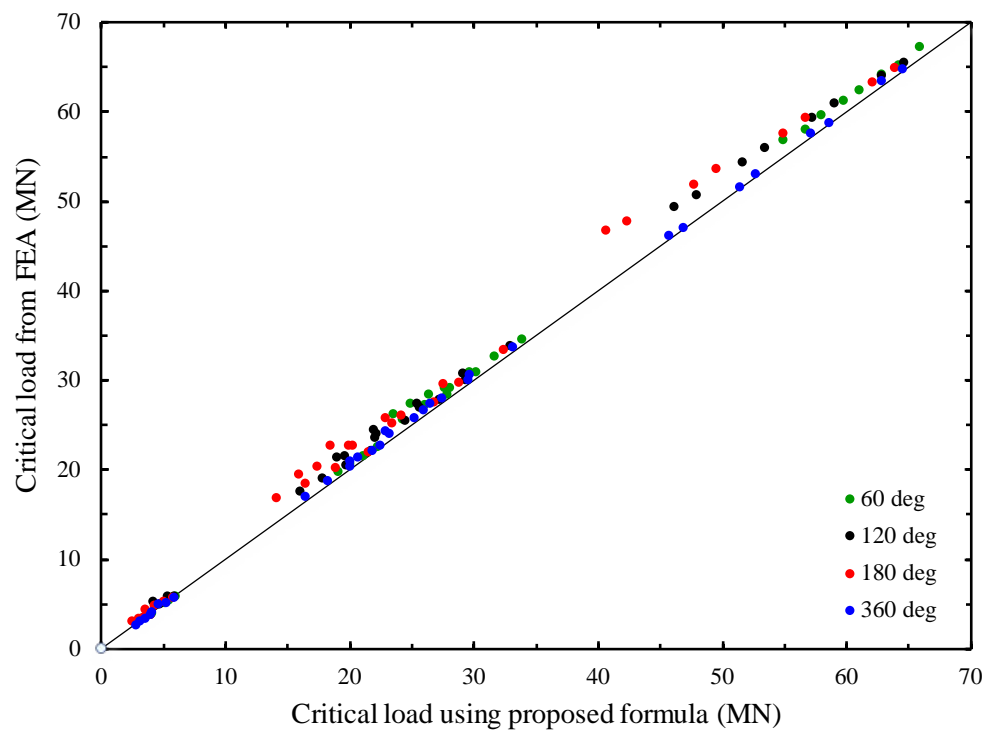


Figure 16. Comparison of critical load from FEA and using proposed formula for patch height $h = L/2$

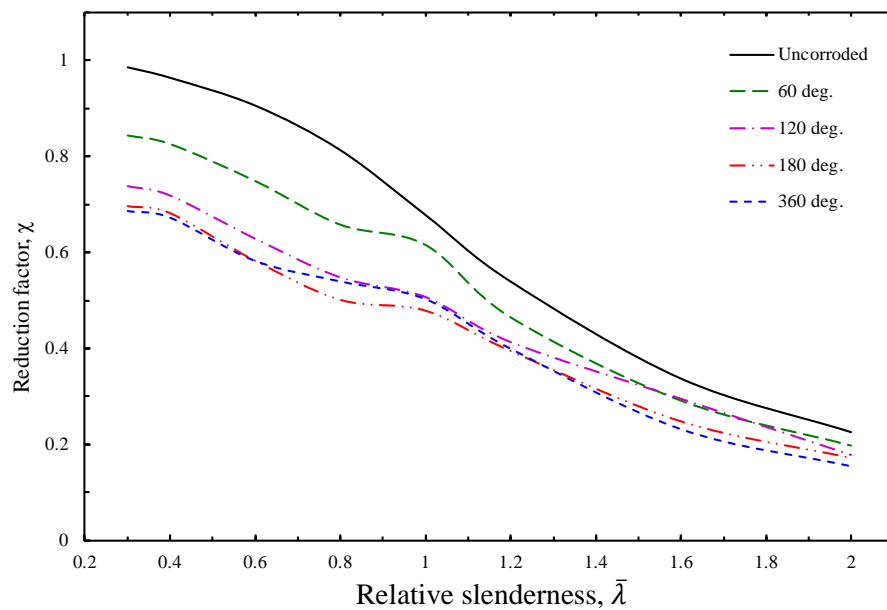


Figure 17. Effect of corrosion patch angle on critical load for $h = L/2$ and $W_a = 10.5$ mm (40 years)

5.3.3. Effect of corrosion thickness wastage on critical load. The maximum reduction of the critical load can be found using the FEA result from uncorroded members and members with corrosion thickness wastage after an age of 40 years ($W_a = 10.5$ mm). This has been found for all the different values for angular extent (θ) of patch, for all the eight members. The results are presented in Table 7 and both the maximum, average reduction and maximum reduction factor (χ_{\max}) for the eight different members is presented. The results from Table 7 shows that the maximum reduction of axial load capacity after 40 years of patch corrosion is 38.3 %, which is a quite significant reduction.

Table 7. Reduction of buckling capacity after 40 years of age

Angle, θ (°)	Maximum reduction of critical load (%)	Average reduction of critical load (%)	Maximum reduction factor, χ_{\max}
60	19.1	14.2	0.657
120	32.5	24.3	0.548
180	38.3	29.8	0.501
360	35.7	30.5	0.582

6. Conclusions

In this paper, a formula is proposed to estimate the buckling capacity of corroded tubular members. This can be used as a tool to evaluate the residual life time of aged offshore structures built with tubular members. The proposed formula is verified with result from FE analyses. It is concluded that patch corrosion significantly reduced the buckling capacity with ageing and that the proposed formula can provide both an accurate and conservative prediction for the buckling capacity of corroded tubular member. The height of the corrosion patch has minor impact on the buckling capacity as buckling occurs in the weakest cross-section. However, both the patch angle and thickness wastage reduce the buckling capacity significantly. Finally, it is concluded that the proposed formula can be easily applied by practicing engineers for a reasonable accurate conservative estimation of residual buckling capacities of corroded tubular members, without the need of any advanced numerical analyses. It is recommended that the proposed formula should be further verified with experimental tests and more numerical analyses.

Acknowledgement

The funding for writing this article is supported by the Program Area for research "COTech - Computational Methods in Offshore Technology" which is founded by Faculty of Science and Technology, University of Stavanger.

References

- [1] Hebor MF and Ricles JM 2002 Local buckling strength of patch corrosion damaged steel tubular bracing *J. Steel Struct.* **2** pp 59-70
- [2] Smith M, Bowley C and Williams L 2002 In situ protection of splash zones - 30 years on *Mat. Perf.* **41** pp 30-33
- [3] Stacey A, Birkinshaw M and Sharp JV 2008 Life extension for ageing offshore installations *Proc. of the 27th Int. Conf. on Off. Mech. and Art. Eng. (Portugal)*
- [4] Aeran A and Gudmestad OT 2017 Guidelines for estimating remaining fatigue life of ageing offshore jacket structures *Proc. of the 36th Int. Conf. Ocean, Off. Artic Eng. (Trondheim)*
- [5] Dong W, Moan T and Gao Z 2012 Fatigue reliability analysis of the jacket support structure for offshore wind turbine considering the effect of corrosion and inspection *Reliability Engineering & System Safety* **106** pp 11-27
- [6] Melchers RE 1999 Corrosion uncertainty modelling for steel structures *J. of Construct. Steel Res.* **52** pp 3-19
- [7] DNV-RP-B401 2010 *Offshore standard DNV-RP-B401: Cathodic protection design* (Det Norske

- Veritas and Germanischer Lloyd SE)
- [8] Faulkner D, Cowling JM and Incecik A 1991 *Integrity of offshore structures* (Glasgow: CRC Press)
 - [9] Nazari M, Khedmati MR and Khalaj FA 2014 A numerical investigation into ultimate strength and buckling behavior of locally corroded steel tubular members *Lat. Am. J. Sol. Struct.* **11**, pp 1063-76
 - [10] Ostapenko A, Wood BA et al 1993 *Residual strength of damaged and deteriorated offshore structures* (Bethlehem: ATLSS Reports)
 - [11] Ostapenko A and Gulec O 1999 *Tubular columns with multiple corrosion patches* (Bethlehem: ATLSS Reports)
 - [12] Lutes LD, Kohutek TL, Ellison BK and Konen KF 2001 Assessing the compressive strength of corroded tubular members *Appl. Ocean Res.* **23** pp 263-68
 - [13] RP 2A-LRFD 1993 *International standard RP 2A-LRFD: Recommended practice for planning, designing and constructing fixed offshore platforms - load and resistance factor design* (American Petroleum Institute)
 - [14] Okada H, Masaoka K, Katsura S and Matsui T 2004 A study of deterioration of strength and reliability of aged jacket structures *Proc. of the OCEANS '04. MTTs/IEEE TECHNO-OCEAN '04 (Kobe)*
 - [15] Yamane M, Tanaka K, Matsuda N, Fujikubo M, Yanagihara D and Iwao N 2006 Residual strength evaluation of corroded steel members in marine environments *Proc. of the 16th Int. Off. Polar Eng. Conf. (San Francisco)*
 - [16] N-006 2015 *Offshore standard N-006: Assessment of structural integrity for existing offshore load-bearing structures* (NORSOK Standard)
 - [17] API RP 2SIM 2014 *API RP 2SIM Recommended Practice for Structural Integrity Management of Fixed Offshore Platforms* (American Petroleum Institute)
 - [18] Boissonnade N, Greiner R, Jaspart JP and Lindner J 2006 *Rules for Member Stability in EN 1993-1-1: Background documentation and design guidelines* (European Convention for Constructional Steelwork)
 - [19] Eurocode 3 2005 *Design of Steel Structures - Part 1-1: General rules and rules for buildings, NS-EN 1993-1-1* (European Standard)
 - [20] ANSYS Meshing User's Guide 2013 (ANSYS Inc.)
 - [21] ISO 19902 2007 *International standard ISO 19902: Fixed steel offshore structures* (European Committee for Standardization)
 - [22] Robertson A 1925 The strength of struts *Selected Engineering Papers* **1** (28)